In Search for Novel $Sn_2Co_3S_2$-based Half-metal Ferromagnets

Florian Pielnhofer, Amadeus Samuel Tragl, Jan Rothballer, and Richard Weihrich

Institut für Anorganische Chemie, Universität Regensburg, Universitätsstr. 31, 93040 Regensburg, Germany

Reprint requests to PD Dr. Richard Weihrich. Fax: 0941/943-4983. E-mail: richard.weihrich@ur.de

Z. Naturforsch. **2014**, *69b*, 55 – 61 / DOI: 10.5560/ZNB.2014-3203
Received July 30, 2013

Substitution effects on magnetism of shandite-type compounds have been studied by density functional theory. The decrease of the Fermi level in the novel half-metallic ferromagnet $Sn_2Co_3S_2$ to higher maxima of the density of states was modeled for substitutions on the Co site by the 3*d* metals Fe, Mn and Cr due to a rigid band scheme. Spin-polarized energy hyper surfaces and densities of states are calculated for $Sn_2Co_3S_2$, and experimentally not yet known $Sn_2Fe_3S_2$, $Sn_2Mn_3S_2$ and $Sn_2Cr_3S_2$ with shandite-type structure. The stability of half-metallic ferromagnetic characteristics, Slater-Pauling behavior, and alternative metastable spin states are discussed.

Key words: Half-metallic Ferromagnet, Shandite, Half Anti Perovskite (HAP), DFT

Introduction

Not only since the discovery of the giant magnetoresistance (GMR) effect and its appreciation with the Nobel prize in 2007 interest arose in ferromagnets for applications in spintronic materials [1, 2]. Half-metal Ferromagnets (HFM) are seen as promising next-generation spintronic compounds. These materials exhibit complete spin polarization as discovered by band structure calculations on Heusler compounds like NiMnSb and Co_2MnSi [3, 4]. Due to their variability in compositions, systematic magnetic design by non-isoelectronic substitution has recently been shown for Heusler compounds [5 – 8]. HFM show a spin-polarized magnetic ground state that is semiconducting for one spin direction (up, α, $\uparrow$). The metallic down-spin direction (β, $\downarrow$) contains additional electrons (type I_A) or holes (type I_B) that are then completely spin-polarized [9 – 12]. As a criterion integer magnetic moments are counted from the difference of electrons in up and down-spin states $M = |n_\alpha - n_\beta|$ and the total number of valence electrons n_{VE} with respect to a semiconducting composition. Easily understood examples are rutile- (TiO_2) type CrO_2 ($n_\alpha - n_\beta = 2$, Cr(+IV), d^2) [12] and pyrite- (FeS_2) type CoS_2 ($n_\alpha - n_\beta = 1$, Co(+II), low-spin d^7) [11, 12].

The recently discovered shandite-type I_A-HFM $Sn_2Co_3S_2$ ($n_\alpha - n_\beta = 1$, $n_{VE} = 47$) [13 – 15] can open new ways for the design of HFM materials. According to experimental and DFT studies it combines high spin polarization with structural and magnetic anisotropy that allows for directional spin coupling [15]. Similar to Heusler compounds, new ways to a magnetic design are possible for shandites due to their variety of compositions [16 – 19]. Increasing the number of electrons by substitution of Co by Ni in $Sn_2Co_3S_2$ leading to $Sn_2Ni_3S_2$ causes a breakdown of magnetism [13, 20]. This is understood from band structure calculations because E_F is shifted towards regions with a broader density of states (DOS). On the other hand, upon reduction of n_{VE} a rigid band scheme applies for semiconducting $InSnCo_3S_2$ ($n_{VE} = 46$, $n_\alpha - n_\beta = 0$) [17]. By further lowering the number of electrons sharp DOS peaks are reached. $In_2Co_3S_2$ ($n_{VE} = 45$) [21] is close to these maxima, but a HFM is not yet realized ($n_\alpha - n_\beta = 0.3$). Subsequently, we probed another way to shift E_F to lower energy, that is by the substitution of Co in $Sn_2Co_3S_2$ by Fe, Mn and Cr. Within a rigid band model this should cause a magnetic destabilization due to the Stoner criterion [22, 23]. This opens up the way to study type I_B HFM that obey a $|n_{VE} - 46|$ rule similar to Heusler compounds. In this paper DFT calculations are reported on hypothetical shandite-type $Sn_2Cr_3S_2$, $Sn_2Mn_3S_2$ and $Sn_2Fe_3S_2$ from scalar relativistic spin-polarized (SP) DFT calculations including predictions on crystal and electronic structures.

Results and Discussion

Crystal and electronic structure concepts

Shandite-type compounds crystallize in space group $R\bar{3}m$ (no. 166) [24]. Fig. 1 shows the respective unit cell of $Sn_2Co_3S_2$ [13] with the simplest representation of the primitive rhombohedral ($a_{rh} = 5.36$ Å, $\alpha_{rh} = 59.9°$) setting. The Sn atoms on Wyckoff positions 1*a* (0, 0, 0) and 1*b* ($^1/_2$, $^1/_2$, $^1/_2$) form a primitive substructure centered by S atoms on 2*b* (*x*, *x*, *x*) with $x = 0.283$ that is also drawn. Metal atoms M = Co are found on 3*c* (0, 0, $^1/_2$) sites. With respect to the SnS substructure, Co atoms occupy half of the S_2Sn_4 tetragonal bipyramids. As a result Co Kagomé layers separate Sn sites between (Sn1, 1*a*) and within (Sn2, 1*b*) the layers. The Co–Co distances (2.68 Å) are longer than in Co metal (2.45 Å) and indicate only weak interactions as compared to the short atomic distances in Kagomé nets of Laves phases. Bonding in $Sn_2Co_3S_2$ is dominated by the coordination of Co in tetragonal bipyramids [CoS_2Sn_4] with Co–S (2.18 Å) and Co–Sn (2.68 Å) bonds. The polyhedra are interlinked by faces within the Kagomé layers and by Sn1 atoms between them [15].

A simple rigid band model for shandites is deduced in Fig. 2 similar to that of Heusler compounds [5, 8]. It is based on quaternary $InSnCo_3S_2$ (46 valence electrons (VE) in 23 fully occupied bands) with a semiconducting ground state [17]. The calculated magnetic moment for $Sn_2Co_3S_2$ is 1.0 μ_B. Compared to semiconducting $InSnCo_3S_2$ this is due to complete spin polarization of one additional electron in the conduction band of the majority spin direction (I_A-HFM [9]), while the minority spin remains semiconducting [14, 15]. Assuming rigid-band and HFM behavior upon substitution by Fe, Mn and Cr, the expected spin states should obey a $|n_{VE} - 46|$ rule (see Table 1). Therein, 46 is the number of valence electrons of semiconducting $InSnCo_3S_2$. It is fulfilled for $Sn_2Co_3S_2$ ($n_{VE} = 47$) with $|47 - 46| = 1.0$.

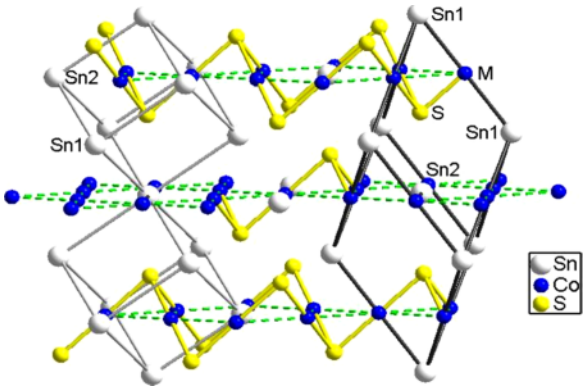

Fig. 1 (color online). Shandite structure with rhombohedral unit cell, Kagomé nets and *A* substructure (*A* = Sn).

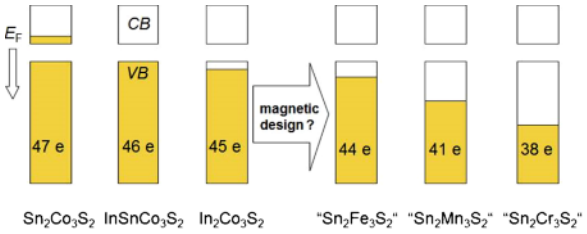

Fig. 2 (color online). Rigid band scheme for different shandite-type compounds, hypothetic compounds in quotes.

Table 1. Calculated lattice parameters for $Sn_2Co_3S_2$ and the hypothetical compounds $Sn_2Fe_3S_2$, $Sn_2Mn_3S_2$ and $Sn_2Cr_3S_2$.

	$Sn_2Co_3S_2$	$Sn_2Fe_3S_2$	$Sn_2Mn_3S_2$	$Sn_2Cr_3S_2$
a_{rh}, Å	5.36	5.46	5.50	5.65
α_{rh}, deg	60.0	58.7	58.8	56.7
V, Å^3	108.9	111.7	114.4	117.8
d_{Sn1-M}, Å	2.68	2.73	2.75	2.83
d_{Sn2-M}, Å	2.68	2.68	2.70	2.68
n_{VE}	47 =	44 =	41 =	38 =
	23 + 24	23 + 21	23 + 18	23 + 15
M_{max}	1	3	5	8

Non-spin-polarized calculations

Within the shandite structure type, lattice parameters and *x*(S) values are predicted by DFT-GGA calculations upon substitution in $Sn_2M_3S_2$ (M = Co, Fe, Mn, Cr). The results for $Sn_2Co_3S_2$ (Table 1) show very good agreement with the experimental data [13]. Due to the angle of $\alpha_{rh} = 60°$ the structure is pseudo cubic. All metal-metal distances are equal ($d_{Sn-Co} = d_{Sn-Co} = d_{Co-Co} = {}^1/_2 a_{rh}$). Increasing lattice parameters a_{rh} and decreasing angles α_{rh} are predicted for $Sn_2M_3S_2$ with M = Co, Fe, Mn, Cr. A similar trend is observed for $In_2Co_3S_2$ ($\alpha_{rh} = 57.9°$) and related to the reduced number of electrons [21]. As a consequence of smaller angles, the *inter*-layer distances become slightly longer than the *intra*-layer metal distances ($Sn_2Fe_3S_2$: $d_{Sn1-Fe} = 2.73$ Å, $d_{Sn2-Fe} = 2.68$ Å).

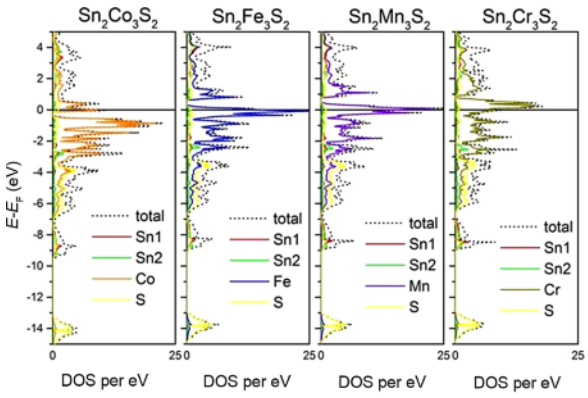

Fig. 3 (color online). NSP-DOS for $Sn_2M_3S_2$ (M = Co, Fe, Mn, Cr).

Table 2. Calculated lattice constants, magnetic states $n_\alpha - n_\beta$, and energy gain for $Sn_2Co_3S_2$ and the hypothetical compounds $Sn_2Fe_3S_2$, $Sn_2Mn_3S_2$ and $Sn_2Cr_3S_2$.

	$Sn_2Co_3S_2$	$Sn_2Fe_3S_2$	$Sn_2Mn_3S_2$	$Sn_2Cr_3S_2$
S1 a_{rh}, Å	5.37	5.45	5.55	5.61
α_{rh}, deg	59.9	58.7	58.8	61.7
V, Å^3	109.3	111.1	117.6	129.3
$n_\alpha - n_\beta$	1.00	2.00	5.00	7.82
S2 a_{rh}, Å		5.60		5.65
α_{rh}, deg		58.7		58.2
V, Å^3		120.5		122.3
$n_\alpha - n_\beta$		6.40		4.37
ΔE_{S1-NSP}, eV	−0.045	−0.361	−1.367	−0.321
ΔV_{S1-NSP}, Å^3	0.4	−0.6	3.2	11.5
ΔV_{S2-S1}, Å^3		9.4		−7.0
ΔE_{S2-NSP}, eV		−0.304		−0.283
ΔE_{S1-S2}, eV		−0.057		−0.038

The band structures obtained from the non-spin-polarized (NSP, Fig. 3) calculations prove that the rigid band model accounts for the chosen hypothetical compounds $Sn_2Fe_3S_2$ (44 VE), $Sn_2Mn_3S_2$ (41 VE) and $Sn_2Cr_3S_2$ (38 VE). The pseudo gap remains at the same position as known for $Sn_2Co_3S_2$ (between valence band no. 23 and 24), and the Fermi level is shifted towards higher DOS maxima upon reduction of the number of VEs. From simple counting of the electrons, maximum magnetic moments of $|n_\alpha - n_\beta| = 1$, 3, 5, and 8 μ_B can be achieved for $n_\beta = 23$.

Spin-polarized calculations

As expected from the aforementioned considerations, spin-polarized ground states (Table 2, S1) are obtained for each of the model compounds. The predicted lattice parameters indicate slight magnetostriction due to increased cell volumes ($\sim 0.5-3\,\%$) as compared to NSP results.

Indeed, the calculated ground states fit the expected values of magnetic moments according to the $|n_\alpha - n_\beta| = |n_{VE} - 46|$ rule for M = Co, Fe, Mn. Due to the integer magnetic moment, they are expected to be of type I_B-HFM [9] as subsequently confirmed by the band structures.

For $Sn_2Cr_3S_2$ the calculated spin polarization (7.8) deviates slightly from the expected value (8.0). Further, the predicted spin-polarized structure shows a strongly increased angle α_{rh}. To study the related peculiarities, spin polarization was also calculated for a larger range of values for the lattice parameters a_{rh} and α_{rh}. The results provide a double-minimum potential with different lattice parameters and spin states. The same is found for $Sn_2Fe_3S_2$. Respective E-V-α_{rh} hypersurfaces are provided in the subsequent discussion of the electronic structures.

$Sn_2Co_3S_2$

In the present systematic investigation the spin state of $Sn_2Co_3S_2$ was also analyzed with respect to the lattice parameters. Fig. 4 confirms the stability of the $S = {}^1/_2$ state found earlier from LDA calculations [13–15]. According to the present GGA investigations the spin-polarized ground state is preferred in energy to the NSP state by 0.045 eV (LDA: 0.025 eV). A compression of the cell volume from $V_{exp} = 110\,$Å^3 to $V < 104\,$Å^3 is necessary to significantly reduce the calculated moment. This confirms a high stability of the $S = {}^1/_2$ ground state. In the DOS plot (Fig. 4b) the I_A-type HFM characteristics [9] are clearly indicated by the non-conducting minority spin channel and the metal majority spin channel. From the spin-polarized DOS the electronic gap is identified between larger and smaller DOS maxima that are attributed to the splitting of Co-3d into t_{2g} and e_g like states according to the coordination of Co.

$Sn_2Fe_3S_2$

$Sn_2Fe_3S_2$ has 44 valence electrons, 3 less than the Co compound. The Fermi energy decreases to the highest maximum of the DOS below the band gap in the NSP case (Fig. 2). Surprisingly not only one, but two

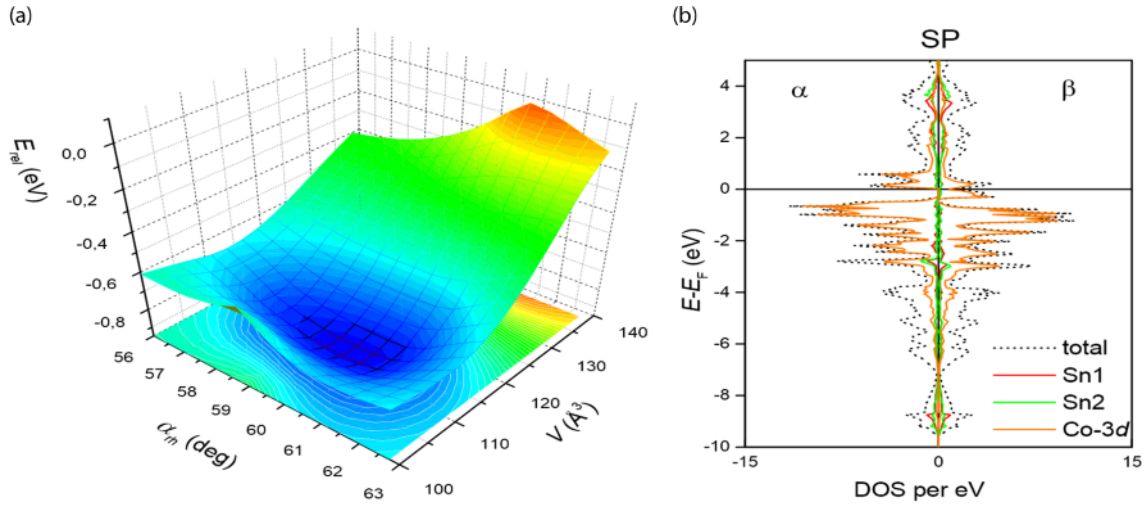

Fig. 4 (color online). $Sn_2Co_3S_2$a) SP E-V-α_{rh} plots and b) DOS for SP ground state.

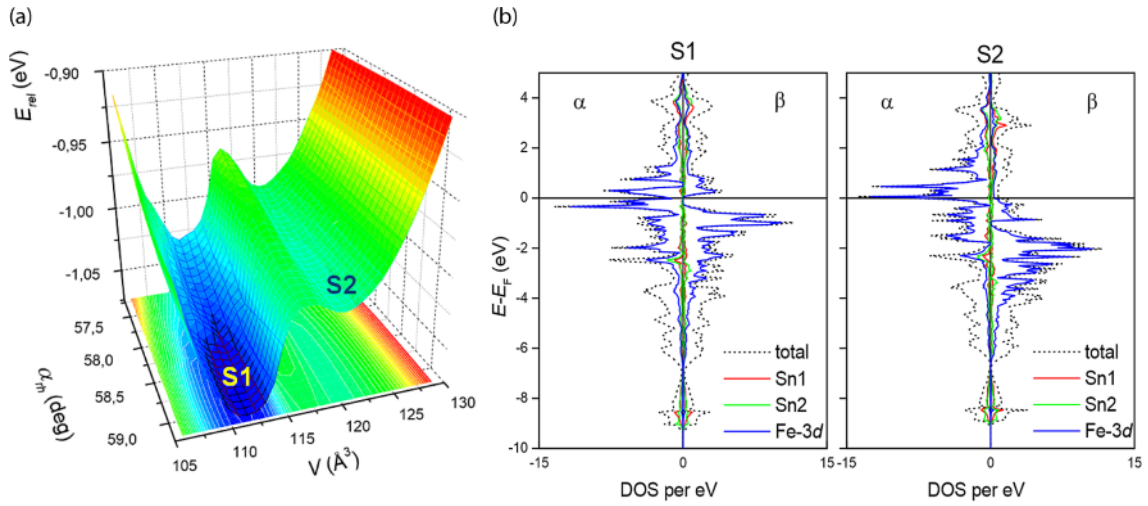

Fig. 5 (color online). a) SP E-V-α_{rh} plots and b) DOS for $Sn_2Fe_3S_2$, different spin states in minima are labeled with S1 and S2.

different spin-polarized states are obtained in SP structural optimizations. The E-V-α_{rh} hypersurface shows two minima at different cell volumes (Fig. 5a). The ground state is located at a cell volume of 111.1 Å^3, similar to $Sn_2Co_3S_2$. The calculated spin difference $n_\alpha - n_\beta = 2.00$ obeys the electron counting rule $|n_{VE} - 46| = n_\alpha - n_\beta = 2$ for $Sn_2Fe_3S_2$. A local by-minimum is identified at the same angle $\alpha_{rh} = 58.7°$, but at a larger cell volume $V = 120.5$ Å^3, and $n_\alpha - n_\beta = 6.40$ is 0.057 eV higher in energy. The ground state S1 is stabilized by $\Delta E_{S1-NSP} = -0.361$ eV. This is one order of magnitude more than for $Sn_2Co_3S_2$. Further, the spin-polarized DOS plot (Fig. 5b) confirms the I_B-HFM characteristics with a semiconducting majority and a metallic minority spin channel. This is identified as Slater-Pauling [25, 26] behavior similar to that of Heusler compounds. Both results confirm the applied concept towards novel magnetic shandites.

The spin state S2 is due to a shift of prominent DOS maxima in the semiconducting channel below E_F. Respective maxima are responsible for the magnetism of $Sn_2Co_3S_2$. One can understand that in non-magnetic

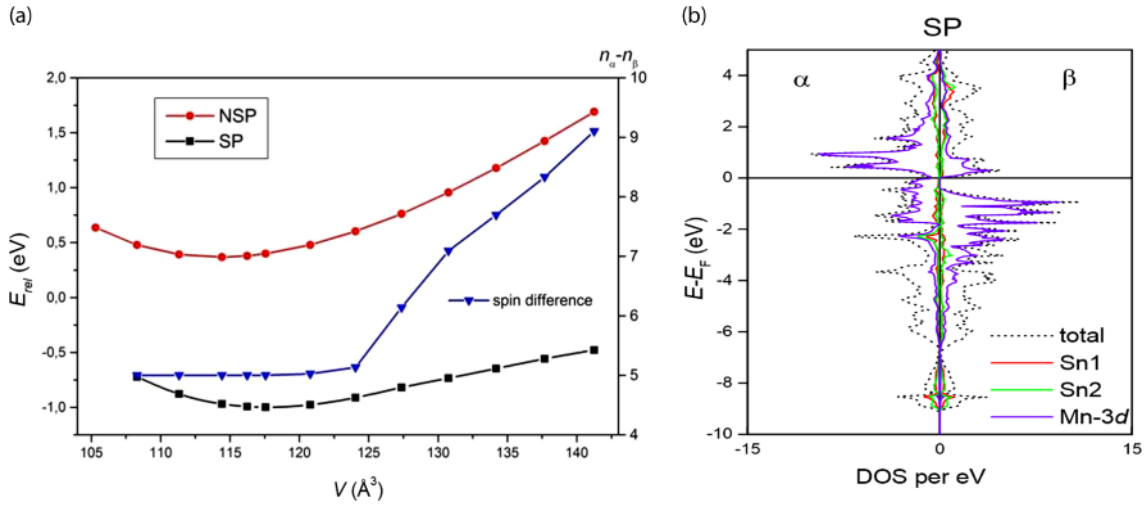

Fig. 6 (color online). a) NSP and SP E-V curves and b) SP-DOS of $Sn_2Mn_3S_2$.

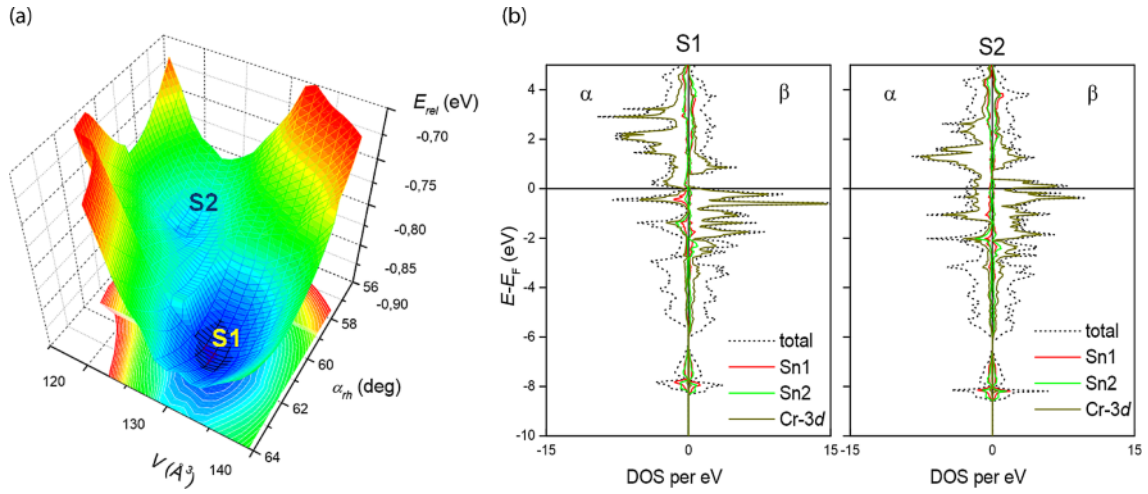

Fig. 7 (color online). a) SP E-V-α_{rh} plots and b) DOS for $Sn_2Cr_3S_2$, different spin states in minima are labeled with S1 and S2.

shandites $Pb_2Ni_3S_2$ and $Sn_2Ni_3S_2$ the Ni-3d bands are fully occupied for both spin channels [24, 27]. As an interesting result, the double minimum potential in the E-V-α_{rh} hypersurface of $Sn_2Fe_3S_2$ serves as model for novel spin crossover materials that might be realized upon doping.

$Sn_2Mn_3S_2$

A further reduction of valence electrons is realized for M = Mn ($n_{VE} = 41$). In the NSP-DOS of $Sn_2Mn_3S_2$ the Fermi energy is located at the high maximum below the gap. The SP ground state is obtained at a cell volume of 117.6 Å^3, which is stabilized by $\Delta E_{SP-NSP} = -1.367$ eV that is about 25 times more than in $Sn_2Co_3S_2$. In contrast to $Sn_2Fe_3S_2$, only one spin-polarized state is found. Similar to $Sn_2Co_3S_2$, the calculations predict a stable spin state upon compression by 5% to $V = 110$ Å^3. For larger cell volumes a sharp increase in magnetic moments is predicted by the present calculations (Fig. 6a). This might indicate a transition to more localized moments and could be

investigated in shandites $A_2M_3X_2$ by substitution with larger A (Pb) or X (Se, Te) site atoms. A similar behavior is found from calculations on $In_2Co_3S_2$ [21].

The SP-DOS is assigned to a HFM state with the Fermi level in the gap of the β-spin channel. Again the counting rule $|n_{VE} - 46| = n_\alpha - n_\beta = 5$ is obeyed for $Sn_2Mn_3S_2$.

$Sn_2Cr_3S_2$

The model compound $Sn_2Cr_3S_2$ consists of 38 valence electrons, and its Fermi level is slightly below the highest maximum in the NSP-DOS, but spin-polarization is also preferred (Fig. 7). In SP structural optimizations two minima appear in the E-V-α_{rh} plot. Here the ground state S1 is at higher cell volume (129.3 Å^3) than the state S2 (117.8 Å^3). S1 is favored in energy by 0.038 eV compared to S2, and by 0.321 eV with respect to the NSP-state. Both minima are located at different angles α_{rh} (S1: 61.7°, S2: 58.2°). From S1 to S2 a barrier of 0.084 eV is indicated. The ferromagnetic ground state of S1 shows DOS characteristics very close to a half-metallic state. The Fermi energy is slightly below the band gap in the β-spin channel. The difference in occupation of spin states $n_\alpha - n_\beta = 7.82$ is very close to the expected value of 8 following the electron counting rule. The DOS of S2 with a spin difference of $n_\alpha - n_\beta = 4.37$ does not show features of a HFM. The different volumes of the states S1 and S2 signal a possible pressure-dependent magnetic transition.

Conclusion

The present DFT investigations were carried out as a support of the search for magnetic design in shandite-type compounds by substitution of the transition metal M. Very similar to Heusler compounds, a simple electron counting rule can be applied to calculate the magnetic moment in $Sn_2Co_3S_2$ and modeled compounds $Sn_2Fe_3S_2$, $Sn_2Mn_3S_2$ and $Sn_2Cr_3S_2$. The Fe and Mn compounds are predicted as half metallic-ferromagnets, and the Cr compound is very close to a HFM state. Both $Sn_2Fe_3S_2$ and $Sn_2Cr_3S_2$ exhibit a double-minimum potential in their E-V-α_{rh} hypersurface. Those minima are attributed to two different spin-polarized states and indicate ways to switch between magnetic states. In the case of $Sn_2Fe_3S_2$ a HFM ground state is obtained, and a state with higher spin difference is located at a greater cell volume. By contrast, the ground state of $Sn_2Cr_3S_2$, which is very close to a HFM, is found at higher cell volumes, and the less stable S2 state at a smaller volume. The modeling of the substituted compounds shows that a systematic decrease of the Fermi level to a higher DOS maximum can lead to other HFM states. The present investigations underline that further substitutions on shandites encompass highly interesting magnetic properties. Future investigations will include the modeling of solid solutions $Sn_2Co_{3-x}M_xS_2$ and $In_2Co_{3-x}M_xS_2$ to achieve a variation of the number of electrons in a tighter region around the dominating DOS maxima.

Experimental Section

Computational details

To determine the lattice parameters of the ground state of the hypothetical shandites, full optimizations of the structure in spacegroup $R\bar{3}m$ have been performed with DFT-GGA calculations. For that purpose 3 parameters, which determine the structure, were optimized in non-spin-polarized (NSP) and spin-polarized (SP) calculations. In the primitive rhombohedral setting the free parameters are given by the lattice parameters a_{rh}, α_{rh} and the positional parameter x(S). The volume of the rhombohedral unit cell is calculated by following Eq. 1:

$$V_{rh} = a_{rh}^3 \cdot \sin\alpha_{rh} \cdot \sqrt{1 - \left(\frac{\cos\alpha_{rh}}{\cos\frac{\alpha_{rh}}{2}}\right)^2} \qquad (1)$$

All calculations were performed in the framework of density functional theory (DFT) with the full potential local orbital (*fplo*, version 9.00-34 [28]) method. The exchange-correlation functional of Perdew, Burke and Ernzerhoff (PBE) [29] of the generalized gradient approximation (GGA) was applied. A set of $12 \times 12 \times 12\,k$ points was used to ensure convergence. The DOS of $Sn_2Co_3S_2$ was calculated using experimental lattice parameters and atomic site postions. All parameters (a_{rh}, α_{rh} and x(S)) were optimized in both NSP and SP calculations on the modeled compounds with Fe, Mn and Cr.

Acknowledgement

The authors thank the Deutsche Forschungsgemeinschaft (DFG) for financial support (WE 4284/1-2) and the Rechenzentrum of the University of Regensburg for computational facilities.

[1] G. Binasch, P. Grünberg, F. Saurenbach, W. Zinn, *Phys. Rev. B* **1989**, *39*, 4828 – 4830.
[2] A. Barthélémy, A. Fert, J.-P. Contour, M. Bowen, V. Cros, J. M. De Teresa, A. Hamzic, J. C. Faini, J. M. Georg, J. Grollier, F. Motaigne, F. Pailloux, F. Petroff, C. Vouille, *J. Magn. Magn. Mater.* **2002**, *242*, 68 – 76.
[3] J. Kübler, *Theory of Itinerant Electron Magnetism*, Oxford University Press, New York, **2000**.
[4] R. A. de Groot, F. M. Müller, P. G. van Engen, K. H. J. Buschow, *Phys. Rev. Lett.* **1983**, *50*, 2024 – 2027.
[5] C. Felser, G. H. Fecher, B. Balke, *Angew. Chem. Int. Ed.* **2007**, *46*, 668 – 699.
[6] V. Alijani, J. Winterlik, G. H. Fecher, S. Shahab Naghav, S. Chadov, T. Gruhn, C. Felser, *J. Phys.: Condens. Matter* **2012**, *24*, 046001 (7 pp).
[7] V. Alijani, S. Ouardi, G. H. Fecher, B. Balke, J. Winterlik, A. Beleanu, X. Kozina, G. Stryganyuk, C. Felser, F. Bernardi, J. Morais, E. Ikenaga, S. Ueda, K. Kobayashi, *Phys. Rev. B* **2011**, *84*, 224416 (10 pp).
[8] T. Graf, S. P. Parkin, C. Felser, *Prog. Solid State Ch.* **2011**, *39*, 1 – 50.
[9] J. M. D. Coey, M. Venkatesan, *J. Appl. Phys.* **2002**, *91*, 8345 – 8350.
[10] G. L. Zhao, J. Callaway, M. Hayashibara, *Phys. Rev. B: Condens. Matter Mater. Phys.* **1993**, *48*, 15781 – 15786.
[11] R. Yamamoto, A. Machida, Y. Moritomo, A. Nakamura, *Phys. Rev. B* **1999**, *59*, R7793–R7796.
[12] K. Schwarz, *J. Phys. F: Met. Phys.* **1986**, *16*, L211 – L215.
[13] R. Weihrich, I. Anusca, *Z. Anorg. Allg. Chem.* **2006**, *632*, 1531 – 1537.
[14] M. Holder, Yu. S. Dedkov, A. Kade, H. Rosner, W. Schnelle, A. Leithe-Jasper, R. Weihrich, S. L. Molodtsov, *Phys. Rev. B* **2009**, *79*, 205116 – 205119.
[15] W. Schnelle, A. Leithe-Jasper, H. Rosner, F. M. Schappacher, R. Pöttgen, F. Pielnhofer, R. Weihrich, *Phys. Rev. B: Condens. Matter Mater. Phys.* **2013**, *88*, 144404-1 – 144404-8.
[16] F. Bachhuber, I. Anusca, J. Rothballer, F. Pielnhofer, P. Peter, R. Weihrich, *Solid State Sci.* **2011**, *13*, 337 – 343.
[17] J. Rothballer, F. Bachhuber, F. Pielnhofer, F. M. Schappacher, R. Pöttgen, R. Weihrich, *Eur. J. Inorg. Chem.* **2013**, *2*, 248 – 255.
[18] I. Anusca, A. Schmid, P. Peter, J. Rothballer, F. Pielnhofer, R. Weihrich, *Z. Anorg. Allg. Chem.* **2009**, *635*, 2410 – 2428.
[19] K. J. Range, F. Rau, M. Zabel, H. Paulus, *Z. Kristallogr.* **1997**, *212*, 50.
[20] T. Kubodera, H. Okabe, Y. Kamihara, M. Matoba, *Physica B* **2006**, *378 – 380*, 1142 – 1143.
[21] F. Pielnhofer, P. Peter, J. Rothballer, W. Yan, F. Bachhuber, F. M. Schappacher, R. Pöttgen, R. Weihrich, *Z. Anorg. Allg. Chem.* **2013**, submitted.
[22] E. C. Stoner, *Proc. R. Soc. London, Ser. A* **1928**, *165*, 372 – 414.
[23] G. A. Landrum, R. Dronskowski, *Angew. Chem. Int. Ed.* **1999**, *38*, 1389 – 1393.
[24] R. Weihrich, S. F. Matar, V. Eyert, F. Rau, M. Zabel, M. Andratschke, I. Anusca, T. Bernert, *Prog. Solid State Chem.* **2007**, *35*, 309 – 20.
[25] J. C. Slater, *Phys. Rev.* **1936**, *49*, 537 – 545.
[26] L. Pauling, *Phys. Rev.* **1938**, *54*, 899 – 904.
[27] P. Gütlich, K. J. Range, C. Felser, C. Schultz-Münzenberg, W. Tremel, D. Walcher, M. Waldeck, *Angew. Chem. Int. Ed.* **1999**, *38*, 2381 – 2384.
[28] K. Koepernik, H. Eschrig, *Phys. Rev. B: Condens. Matter Mater. Phys.* **1999**, *59*, 1743 – 1757.
[29] J. P. Perdew, K. Burke, M. Ernzerhoff, *Phys. Rev. Lett.* **1996**, *77*, 3865 – 3868.